



# Thermo-Radiative Cell – A New Waste Heat Recovery Technology for Space Power Applications

Jianjian Wang<sup>1</sup>, Chien-Hua Chen<sup>2</sup>, Richard Bonner<sup>3</sup>, and William G. Anderson<sup>4</sup>

*Advanced Cooling Technologies, Inc., Lancaster, PA 17601 USA*

In order to satisfy the long-lasting and high energy/power density requirements for NASA deep space exploration missions, Pu-238 has been identified as one of the most suitable radioisotope fuels for GPHS modules since the 1960s. The availability of Pu-238 is currently extremely limited. The limited availability suggests that efficiently using the heat generated by the GPHS is very important and critical for NASA space applications. However, the efficiency of the most widely used radioisotope thermoelectric generators is only about 6-8%, which means that a significant amount of energy is dissipated as waste heat via radiators such as metallic fins. In deep space, the extremely cold universe (3 K) provides a robust heat sink. Even for a heat source with a temperature below 373 K, the corresponding Carnot efficiency can be more than 99%. In this paper, we show a proof-of-concept demonstration of using a thermo-radiative cell, a new technology concept conceived in 2015, to convert heat to electricity. A reversed I-V characteristic between thermo-radiative cell and photovoltaic cell is also experimentally demonstrated for the first time. The predicted efficiency of thermo-radiative cells is significantly higher than thermoelectrics at peak power output, and can be even higher at reduced power output. Integrating thermo-radiative cells with radioisotope heating units (high-grade heat) or radioisotope power system (RPS) radiators (low-grade waste heat) could provide a new way to significantly increase the energy efficiency of Pu-238 or other radioisotope fuels. Preliminary calculations indicate that when combining the thermo-radiative cells with RPS radiators, the thermoelectric RPS efficiency could be increased from 6% to 10-14%, and the dynamics RPS efficiency could be increased from 28% to 34-47%, depending on the radiator temperature.

## I. Nomenclature

$c$	=	speed of light in vacuum, [m/s]
$e$	=	elementary charge, [C]
$h$	=	Planck's constant, [J · s]
$k_B$	=	Boltzmann constant, [J/K]
$\eta$	=	thermo-radiative cell efficiency
$\varepsilon$	=	photon energy, [eV]
$E_g$	=	semiconductor band gap, [eV]
$\dot{E}_{rad}$	=	radiative energy flux emitted by the cell, [W/m <sup>2</sup> ]

<sup>1</sup> Research & Development Engineer II, R&D Department

<sup>2</sup> Lead Engineer, R&D Department

<sup>3</sup> Vice President of R&D, R&D Department

<sup>4</sup> Chief Engineer, R&D Department

$\dot{E}_{abs}$	= radiative energy flux absorbed by the cell, [W/m <sup>2</sup> ]
$P_e$	= power density of thermo-radiative cell, [W/m <sup>2</sup> ]
$I$	= electrical current, [A]
$V$	= cell voltage, [volts]
$Q_{in}$	= thermal power input per unit cell surface area, [W/m <sup>2</sup> ]
$T_a, T_c$	= ambient temperature, cell temperature, [K]

## II. Introduction

Traditionally, there are two classes of thermal-to-electrical energy conversion systems: static and dynamic. The key benefit of static thermal-to-electrical energy conversion systems, like thermoelectrics, thermophotovoltaics, and thermionics, is that no moving parts are involved in the system. Dynamic thermal-to-electrical energy conversion systems, like Stirling, Brayton and Rankine cycle engines, involve repetitive motion of moving parts containing various working fluids. The operation of these thermal-to-electrical energy conversion systems in deep space requires a high temperature heat source which is usually supplied by General Purpose Heat Source (GPHS) modules (Figure 1a). In order to satisfy the long-lasting and high energy/power density requirements for the deep space exploration missions, Pu-238 has been identified as the most suitable radioisotope fuel for GPHS modules since the 1960s [1].

However, the bulk production of Pu-238 in the US was stopped in 1988. Although DOE is expected to be able to produce 1.5 kg Pu-238 per year by 2025 for NASA, there are still many uncertainties, and DOE is facing many challenges to meet this production goal. In addition, due to the highly technical nature of the Pu-238 production process and the long time required (~2 years) for technical staff training, the unit price of Pu-238 is very high, ~\$8 million per kilogram [2,3]. NASA's budget can only support one radioisotope power system (RPS) mission every 4 years [3]. The extremely limited availability and high cost of Pu-238 suggest that efficiently using the heat generated by the GPHS is very important and critical for NASA space applications. However, the efficiency of multi-mission radioisotope thermoelectric generator (Figure 1b), which is a thermoelectric RPS, is only about 6%. Even though the dynamic thermal-to-electrical energy conversion systems (e.g. advanced Stirling radioisotope generator, Figure 1c) can achieve 25% or even higher efficiency, there is still a significant amount of energy dissipated as wasted heat via radiators such as metallic fins. Harvesting energy from this waste heat not only improves the total energy utilization efficiency of GPHS, but also significantly reduces the mass of the required RPS. For example, one of the technologies that NASA is developing to increase the RPS efficiency is called the e-MMRTG, which could increase the efficiency from 6% to 8%. According to NASA officials [3], for a mission requiring 300 W of power, only two e-MMRTGs are needed instead of three MMRTGs. This could save about 3.5 kg Pu-238 and reduce the mission overall weight by 45 kg, which is a tremendous cost saving considering that the cost of a MMRTG is about \$77 million.

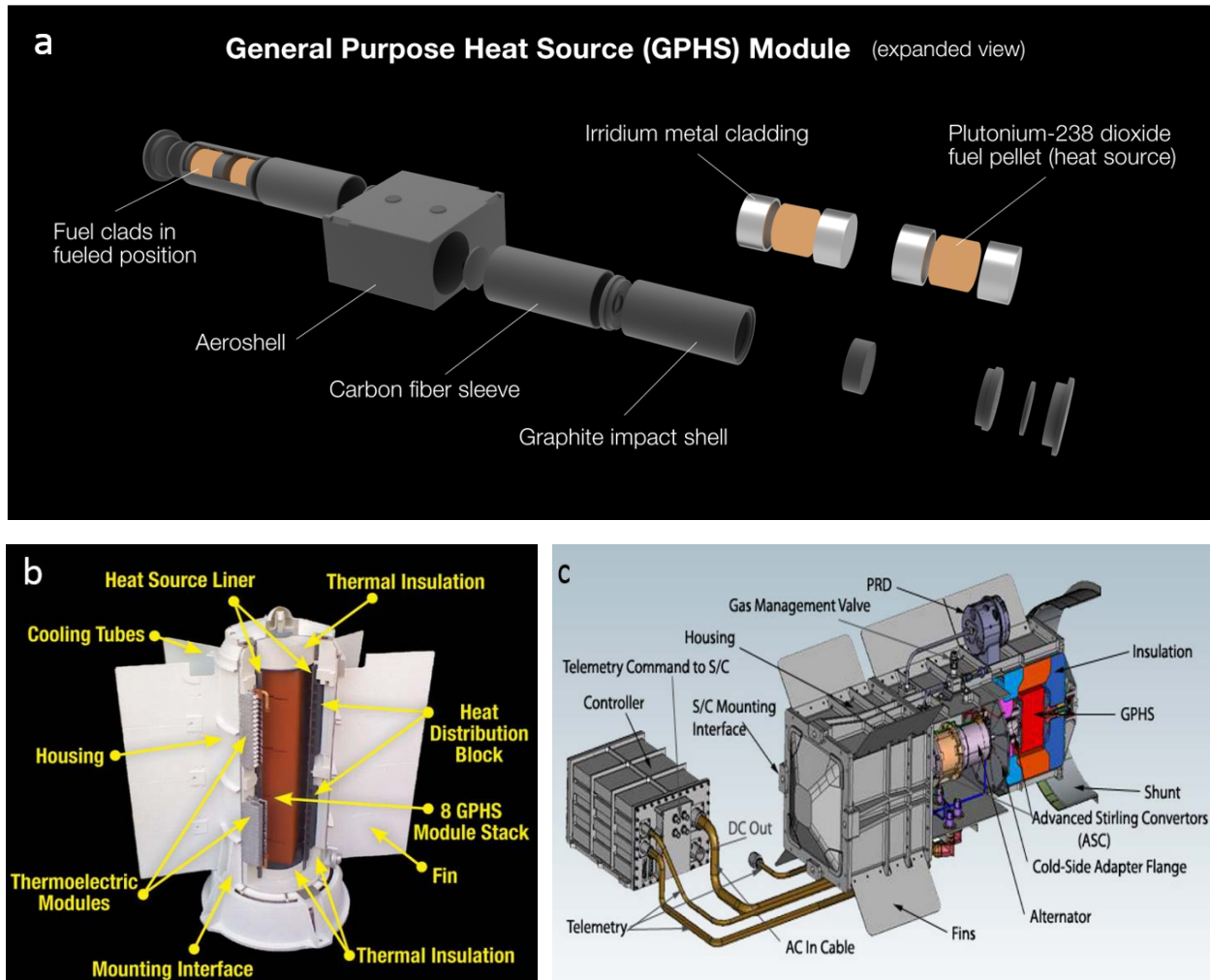


**Figure 1: a) GPMS; b) Multi-Mission Radioisotope Thermoelectric Generator (MMRTG) used for powering the Mars Science Laboratory rover, Curiosity; c) Advanced Stirling converter. (Images courtesy of NASA.gov)**

For any thermodynamic energy conversion system, from ideal Carnot heat engine to photovoltaics, thermophotovoltaics, thermionics, or thermoelectrics, there must be a high temperature heat source and a low temperature heat sink. For the aforementioned energy conversion processes, the heat source temperature ranges from 800-1200 K in thermoelectrics to near 5800 K in photovoltaics. The high temperature in these heat sources is necessary due to the relatively high temperature heat sinks (~300-500 K) used in these energy converters since larger temperature differences between the heat source and heat sink usually give higher energy conversion efficiency. In deep space, the extremely cold background temperature of around 3 K provides a robust heat sink. Even for a waste heat source with a temperature below 373 K, the corresponding Carnot efficiency can be more than 99%. Here we are imagining an energy converter that can convert part of the waste heat from the primary converters to electricity and dump the rest of the waste heat into deep space by radiation (the only choice to reject heat in this deep space). Such a device belongs to the general emissive energy harvester (EEH) which was proposed by Byrnes *et al.* in 2014 [4]. The EEH is a device that has high emissivity in the “atmospheric window” at 8-

13  $\mu\text{m}$  and low emissivity for other wavelengths. Since the atmosphere is almost transparent for radiation wavelengths between 8  $\mu\text{m}$  and 13  $\mu\text{m}$ , the earth's surface temperature is 275-300 K and the outer space temperature is only 3 K, so the EEH (at the earth's ambient temperature) will emit far more thermal radiation than it receives from the outer space. The imbalance of the emitted and the absorbed thermal radiation can be converted into an imbalance of charge carrier motion in the EEH, i.e., generating electricity (Figure 2). Based on this general EEH idea, Strandberg [5] proposed a new technology concept, termed the thermo-radiative cell, to convert heat into electricity and reject the unused heat via thermal radiation.

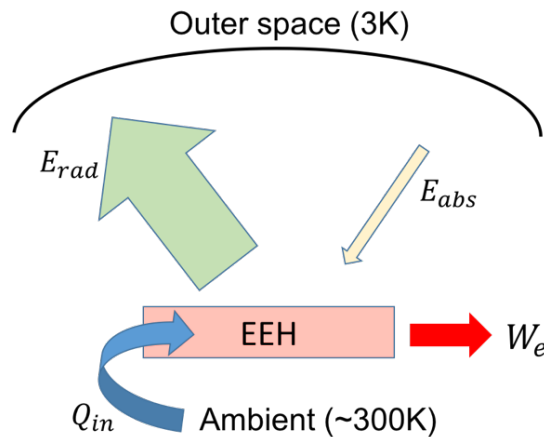


**Figure 2: Principle of emissive energy harvester (EEH).**

### III. Comparison of Thermo-radiative Cell and Photovoltaic Cell

The thermo-radiative cell, which can be used for NASA deep space applications to convert waste heat into electricity, is made of semiconductor P-N junctions and operated at an elevated temperature (325 K to 475 K, or even higher temperature depends on the accessible waste heat source temperature) compared to its surroundings (3-150 K in cold universe). It is well-known that P-N junctions are widely used in photovoltaic (PV) cells to convert solar radiation energy to electric power. In a photovoltaic cell, since the solar surface temperature is much higher than the cell temperature, more photons are absorbed by the PV cell than emitted by the PV cell. If the absorbed photon energy is larger than the semiconductor bandgap  $E_g$  (e.g., 1.1 eV for silicon), the photon can excite an electron from the valence band (where the electron is bounded) to the conduction band (where electron can move almost freely), i.e., generating an electron-hole pair. The excess energy of the photon will be dissipated quickly as heat. At the open circuit condition, the high photon flux causes the electron-hole pair generation rate to be much higher than their initial recombination rate. As the electron-hole pair concentration increases, their recombination rate also increases. The excessive electron concentration raises the electron quasi-Fermi energy in the n-type semiconductor part, while the excessive hole concentration lowers the hole quasi-Fermi energy in the p-type semiconductor part. The splitting of these quasi-Fermi energies in the n-type and p-type parts corresponds to the built-up of a positive voltage in the device [6]. This voltage increases to a stable value when the electron-hole pair generation rate equals to their recombination rate. For photovoltaic cells, the photo-to-electrical energy conversion occurs at the cold side of this thermodynamic process.

The working principles of the thermo-radiative (TR) cell are closely related to the working principle of photovoltaic cell, except they work in reverse. In a thermo-radiative cell, the surrounding temperature is

lower than the cell temperature, thus the electron-hole pair generation rate is slower than the recombination rate. The insufficient electron concentration lowers the electron quasi-Fermi energy in the n-type semiconductor part, while the insufficient hole concentration raises the hole quasi-Fermi energy in the p-type semiconductor part. This results in a negative voltage built-up in the device. When the device is connected with a load, the current direction in the thermo-radiative cell is also opposite to that of a photovoltaic cell (Figure 3). For thermo-radiative cells, the thermal-to-electrical energy conversion occurs at the hot side of this thermodynamic process.

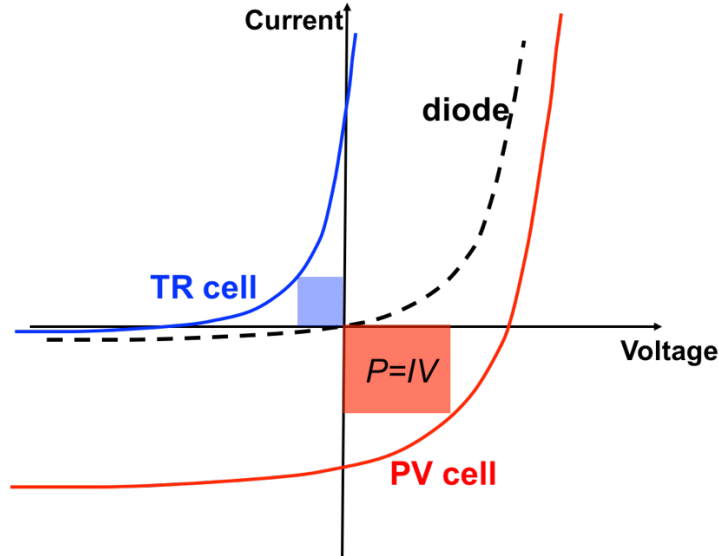


**Figure 3: The voltage and current direction in PV and TR cells are opposite, but both can generate electrical power ( $P=IV < 0$ ).**

#### IV. Theoretical Model

Power density and energy efficiency are the two most important parameters for any power generation devices. For deep space applications, the heat sink temperature can vary from 3 K (when the TR cell faces the deep space) to 100-150 K (when the TR cell faces some cold planets or their satellites). The power density of the thermo-radiative cell increases with the heat source temperature. The efficiency of the thermo-radiative cell varies with the cell voltage or the power density. The efficiency of the thermo-radiative cell can be analyzed by the principle of detailed balance, which Shockley and Queisser used to derive the famous Shockley-Queisser limit [7] for photovoltaic cell. The thermo-radiative cell efficiency  $\eta$  is defined as

$$\eta = \frac{P_e}{Q_{in}} = \frac{P_e}{P_e + \dot{E}_{rad} - \dot{E}_{abs}}, \quad (1)$$

where  $P_e$  is the generated electrical power per unit cell area, i.e., power density of the thermo-radiative cell,  $Q_{in}$  is the thermal energy supplied to the cell per unit time,  $\dot{E}_{rad}$  is the radiative energy flux emitted from the cell surface, and  $\dot{E}_{abs}$  is the radiative energy flux received by the cell.

The power density  $P_e$  can be calculated as [5, 8]

$$P_e = IV = eV \left( \frac{2\pi}{h^3 c^2} \right) \left[ \int_{E_g}^{\infty} \frac{\varepsilon^2}{\exp\left(\frac{\varepsilon}{k_B T_a}\right) - 1} d\varepsilon - \int_{E_g}^{\infty} \frac{\varepsilon^2}{\exp\left(\frac{\varepsilon - qV}{k_B T_c}\right) - 1} d\varepsilon \right], \quad (2)$$

where  $e$  is the elementary charge,  $V$  is the cell voltage,  $h$  is Planck's constant,  $c$  is the speed of light in vacuum,  $E_g$  is the band gap of the semiconductor used for the thermo-radiative cell,  $k_B$  is the Boltzmann constant,  $T_c$  is the cell temperature,  $T_a$  is the ambient temperature, and  $\varepsilon$  is the photon energy.

The radiative energy fluxes  $\dot{E}_{rad}$  and  $\dot{E}_{abs}$  are given by [5, 8]

$$\dot{E}_{rad} = \frac{2\pi}{h^3 c^2} \int_{E_g}^{\infty} \frac{\varepsilon^3}{\exp\left(\frac{\varepsilon - qV}{k_B T_c}\right) - 1} d\varepsilon, \quad (3)$$

$$\dot{E}_{abs} = \frac{2\pi}{h^3 c^2} \int_{E_g}^{\infty} \frac{\varepsilon^3}{\exp\left(\frac{\varepsilon}{k_B T_a}\right) - 1} d\varepsilon, \quad (4)$$

The above theoretical model can be used to analyze the power density and efficiency of the thermo-radiative cell at different operating temperatures. The heat sink temperature is assumed to be 3 K (facing deep space) in our calculations. In fact, for a heat sink temperature of 3-150 K in the universe, the radiation emitted by the heat sink is negligible compared with the radiation emitted by a thermo-radiative cell at a temperature above 323 K (or 50 °C), due to the 4<sup>th</sup> power of temperature dependence for radiation. The temperature range of typical RPS radiators is about 325-475 K. Therefore, it does not show any difference in the thermo-radiative performance when the heat sink temperature changes from 3 K to 150 K.

Assuming a thermo-radiative cell with a bandgap 0.1 eV (typical long-wavelength infrared (LWIR) photodetector materials,  $\text{Hg}_{1-x}\text{Cd}_x\text{Te}$  and  $\text{InAs}_{1-x}\text{Sb}_x$ , could have this low bandgap when appropriate Cd and Sb composition percentages are chosen), its output power density when harvesting electricity from low-grade waste heat (350 K, 425 K and 500 K) is calculated and shown in Figure 4. In this temperature range, the maximum power density ranges from several tens of Watts per square meter to a few hundred Watts per square meter. For thermo-radiative cells operating at 500 K (near the low-grade waste heat upper limit), the generated electrical power density can be as high as 240 W/m<sup>2</sup> (red curve in Figure 4), which is on the same order of magnitude as a photovoltaic cell. When the cell temperature reaches 700 K (medium-grade waste heat), the generated power density could be above one thousand Watts per square meter (blue curve in Figure 4), which is several times higher than the state-of-the-art power density achieved in photovoltaic cells. The generated electricity could be used to supply power for the power electronics on NASA spacecraft.

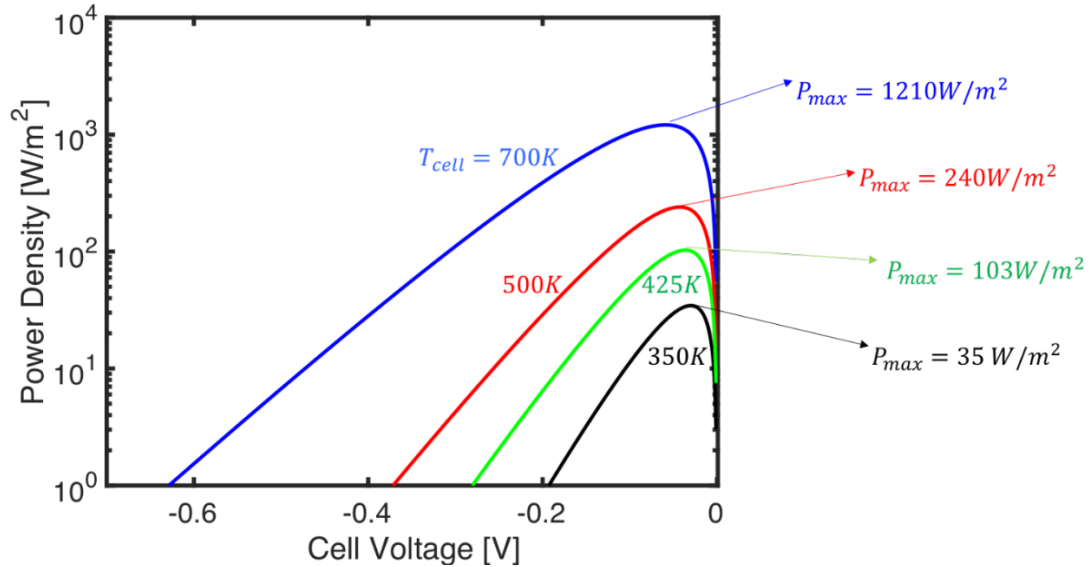


**Figure 4:** The electrical power density of the thermo-radiative cell as a function of cell voltage at different operation temperatures (350 K, 425 K, 500 K, and 700 K). These calculations assume the heat sink is deep space at 3 K and the cell bandgap is 0.1 eV.

Accordingly, the efficiency of the thermo-radiative cell operating at the same conditions as Figure 4 is calculated and shown in Figure 5. Although the thermo-radiative cell efficiency increases with the magnitude of the cell voltage, the power density generated at those very large efficiency ranges (e.g., >50%) is low, except when the thermo-radiative cell is operated at relatively higher temperature (e.g., 700 K). Therefore, the efficiency near those peak power outputs is more useful (10%-35%). For low-grade waste heat recovery, the efficiency at peak power output is above 12%, which is significantly higher than the 6-8% efficiency of state-of-the-art thermoelectric RPS.

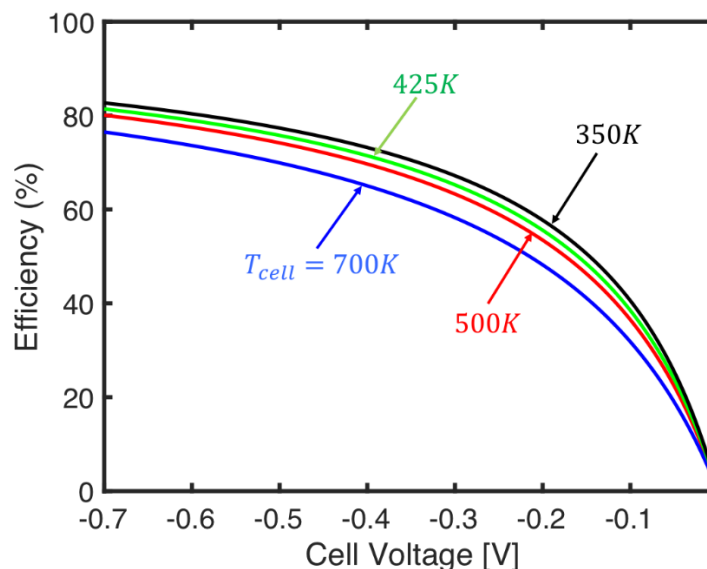


**Figure 5:** The efficiency of the thermo-radiative cell as a function of cell voltage at different operation temperatures (350 K, 425 K, 500 K, and 700 K), assuming the heat sink is deep space at 3 K and the cell bandgap is 0.1 eV.

It should be noted that the efficiency (at maximum power output) and power density calculated above can be exceeded if the thermo-radiative cell spectral emittance is well-designed. For example, for a thermo-radiative cell operating at 300 K and radiating to a heat sink at 3 K, Santhanam et al. [9] calculated the multispectral limit of its power density to be about 55 W/m<sup>2</sup>, which is significantly higher than the calculation in Figure 4. Hsu et al. [6] calculated that with a narrow-band selective emission surface, the thermo-radiative cell efficiency can be further increased.

## V. Experimental Demonstration

### A. Thermo-Radiative Cell System Setup

For NASA space applications, the extremely cold universe (3 K) will serve as the heat sink for the thermo-radiative cell energy conversion process. However, achieving such low temperature is difficult and requires expensive equipment. For terrestrial proof-of-concept demonstration experiments, liquid nitrogen-based heat sink is chosen to mimic the cold universe. The radiation power from a black surface is proportional to the 4<sup>th</sup> power of temperature. For a heat sink ( $T_{sink}$ ) at either 77 K or 3 K and a thermo-radiative cell at a given temperature ( $T_{cell}$ ), as long as  $T_{cell}^4 \gg T_{sink}^4$ , the net outgoing radiation (emitted minus absorbed) power from the thermo-radiative cell surface is the same for both cases. Therefore, it is accurate enough to mimic the cold universe heat sink with liquid nitrogen-base cryogenic system. The thermo-radiative cell is kept near room temperature or mildly heated to a temperature corresponding to the typical low-grade waste heat temperature (less than 100°C).

The thermo-radiative cell performs best with low bandgap semiconductors. There are a few good semiconductor candidates that are commercially available and suitable for working as thermo-radiative cells for low-grade waste heat recovery. These candidates are InSb, Hg<sub>1-x</sub>Cd<sub>x</sub>Te, and InAs<sub>1-x</sub>Sb<sub>x</sub>, with appropriate x. Usually the bandgap  $E_g$  of semiconductors decreases with temperature. Therefore, for high temperature operation, there are more semiconductor choices (e.g., InAs). Hg<sub>1-x</sub>Cd<sub>x</sub>Te (MCT) commercial photodiode has been selected as the thermo-radiative cell in this demonstration, due to its wide tunable bandgap range and commercial availability.

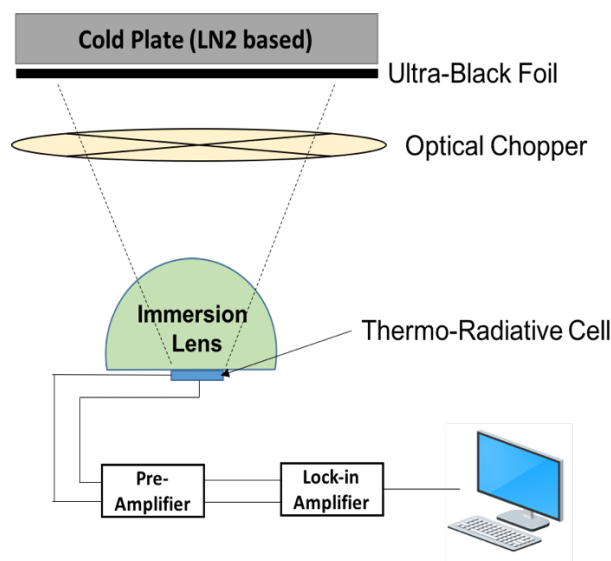
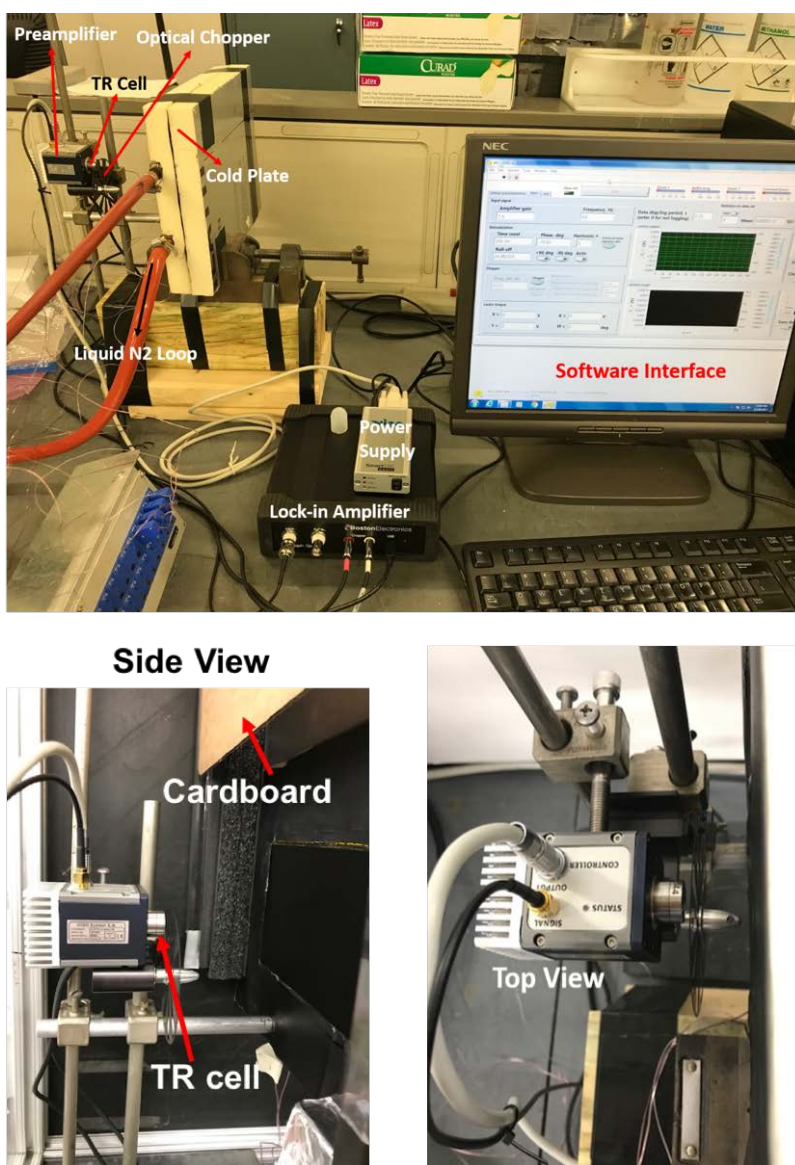


Figure 6: Schematic design of thermo-radiative cell measurement system.

The HgCdTe photodiode we used is covered with an immersion lens (Figure 6) so that the field of view (FOV) can be controlled (e.g.,  $35^\circ$  in our experiment). Therefore, it is not necessary to use a hemispherical cryogenic surface or a planar cryogenic surface placed very close to the cell. We placed a planar cold plate (liquid nitrogen cooled) at a finite distance from the cell and ensure that cold plate surface completely covers the FOV of the HgCdTe thermo-radiative cell (Figure 6). The cold plate is made of aluminum with embedded copper tubes. Liquid nitrogen flows through the copper tubes to maintain the aluminum plate surface at low temperature. The surface temperature is adjustable from room temperature down to around 77 K. The surface temperature (four thermocouples placed on the surface of cold plate) is controlled by the flow rate of the liquid nitrogen in the copper tube. An ultra-black foil is covered on the top surface of the cold plate. It aims to minimize the reflections from the environment to the thermo-radiative cell since it has very low reflectance from visible light to long-wavelength infrared (LWIR).



**Figure 7: Integrated thermo-radiative cell measurement system.**

Figure 7 shows the integrated thermo-radiative cell measurement system. During the measurements, a cardboard sheet is controlled manually to block/unblock the view of the thermo-radiative cell. The system is placed in a chamber during the measurement which is flowed with dry nitrogen gas to maintain a positive pressure and reduced humidity inside, which could avoid the water vapor in the ambient entering into the chamber as well as minimize the condensation on the cold plate.

## B. Thermo-Radiative Cell On/Off Response Demonstration

Initially, the cell and the cold plate are both at ambient temperature. At this point, there should be zero net radiation from the thermo-radiative cell to the cold plate. The measured output electrical signal of the thermo-radiative cell is almost zero as expected. As we continuously decrease the cold plate surface temperature by controlling the liquid nitrogen flow rate, the output electrical signal continuously increases. If we use cardboard to suddenly block the view of the cell to the cold plate, we observed that the electrical signal suddenly drops to zero. This is because the cardboard and the thermo-radiative cell are at the same temperature. In other words, the thermo-radiative cell changes from the “ON” state when it faces to the low temperature cold plate, to the “OFF” state when it suddenly faces to the ambient temperature cardboard. This ON/OFF response is clearly showed in Figure 8.

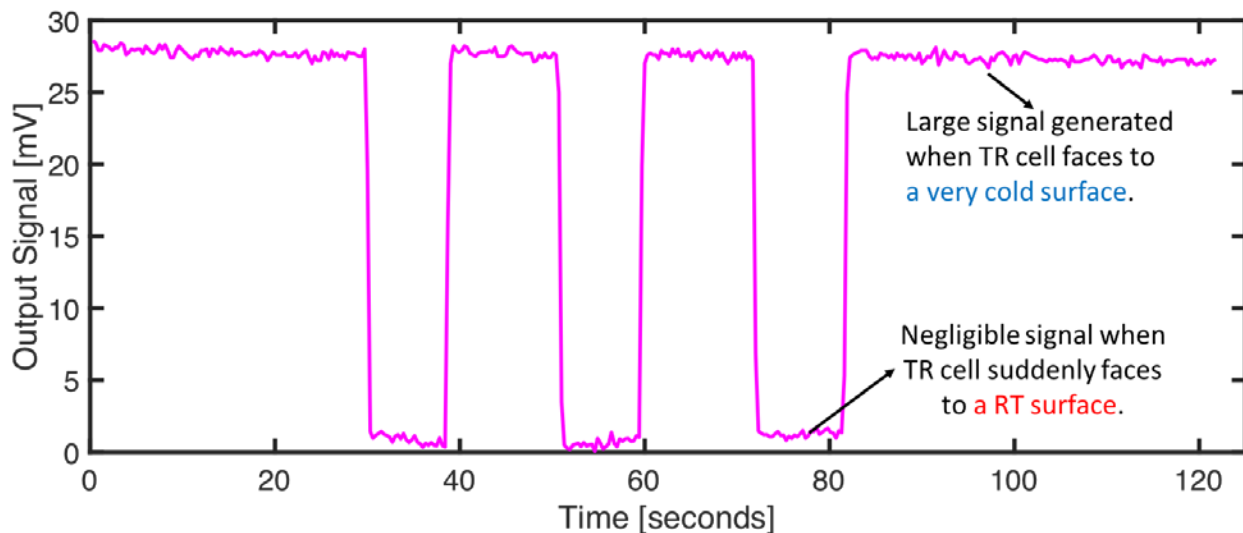


**Figure 8:** An example measurement curve when the cold plate temperature is  $-50\text{ }^{\circ}\text{C}$  and the thermo-radiative cell is at ambient temperature. A large signal is observed when the thermo-radiative cell faces to the very cold surface (ON state). A negligible signal is observed when the cell suddenly faces to the ambient temperature cardboard (OFF state).

If the aluminum plate is heated to above ambient temperature by changing the liquid nitrogen flow to hot water flow, then the net radiation is from the environment to the cell. The cell will work like a photovoltaic cell, or more precisely, a thermophotovoltaic (TPV) cell. Therefore, we conducted two sets of experiments for comparison. In the first set, the plate temperature is changed from ambient to  $-150\text{ }^{\circ}\text{C}$ , i.e., the cell works in the thermo-radiative cell mode. The output signal increases from  $0.3\text{ mV}$  to  $29.2\text{ mV}$ . In the second set, the plate temperature is changed from ambient to  $80\text{ }^{\circ}\text{C}$ , i.e., the cell works in the (thermo-)photovoltaic cell mode. The output signal increases from  $0.3\text{ mV}$  to  $81.1\text{ mV}$ . In both cases, the cell is at ambient temperature  $295\text{ K}$ . Given the trans-impedance amplifier (the pre-amplifier) gain, we

converted the output voltage signal back to the short-circuit current, and plot the results in Figure 9. The short-circuit current is saturated around  $3 \mu\text{A}$  when the cold plate temperature is below 200 K. This is consistent with previous analysis, that as long as the heat sink temperature is below 200 K, the generated electrical power shows negligible difference since  $T_{cell}^4 \gg T_{sink}^4$ . It should be mentioned that the physical area of the thermo-radiative cell is only  $0.01 \text{ mm}^2$ . Thus, the saturated current density is about  $300 \text{ A/m}^2$ , which is similar to typical terrestrial commercial solar cell current density.

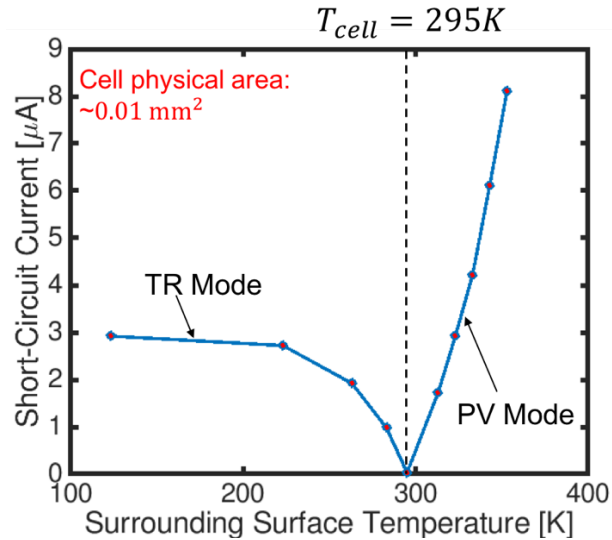


**Figure 9:** The cell short-circuit current as a function of the plate temperature. When the plate temperature is below ambient, the cell works in the TR mode. When the plate temperature is above ambient, the cell works in the PV (or TPV) mode. Note the cell area is only  $0.01 \text{ mm}^2$ , therefore,  $3 \mu\text{A}$  in the figure means  $300 \text{ A/m}^2$ .

### C. Thermo-Radiative Cell Current-Voltage Characteristic Demonstration

The thermo-radiative cell bandgap in the above ON/OFF response is about 0.21 eV. Because the pre-amplifier is integrated with the cell and they cannot be separated from each other, another HgCdTe photodiode was purchased for the current-voltage characteristics measurements. This thermo-radiative cell has a bandgap around 0.32 eV. This bandgap is a little too large for low-temperature heat operation. However, it can still be used as a thermo-radiative cell, except that the short-circuit current of this second cell will be much smaller than the first cell. Figure 10 shows the experimental configuration for the thermo-radiative cell current-voltage characteristics measurements. The major difference compared with the previous ON/OFF response experiment is that the thermo-radiative cell can now be heated by the thin film heater wrapped around it. The I-V curve is measured by Keithley SourceMeter 2450. The cell is still facing to the cold plate covered by the ultra-black foil. The temperature of the plate can be controlled by liquid nitrogen or hot water.

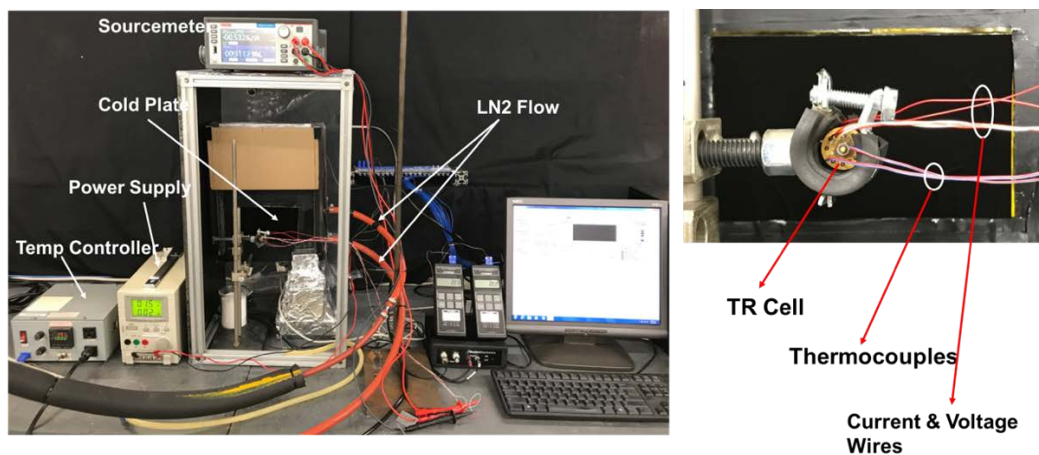


**Figure 10: Experimental configuration for the thermo-radiative cell I-V measurements.**

We compared the I-V curves of the cell under three different conditions. Under the first condition, the cell is in thermal equilibrium with the ambient. In this case, the I-V curve passes through the origin point, i.e., when the bias  $V = 0$ , the current  $I = 0$  (see the blue curves in Figure 11). The cell shows the standard p-n junction behavior under dark condition. As we heated up the cell and controlled the plate to the cryogenic temperature, the cell works in the thermo-radiative cell mode. The I-V curve moves upwards from the thermal equilibrium curve, i.e., when the bias  $V = 0$ , the short-circuit current is positive (see the black curves in Figure 11). When we kept the cell at ambient temperature and heated up the plate temperature, the cell works in the photovoltaic mode. The I-V curve moves downwards from the thermal equilibrium curve, i.e., when the bias  $V = 0$ , the short-circuit current is negative (see the red curves in Figure 11).

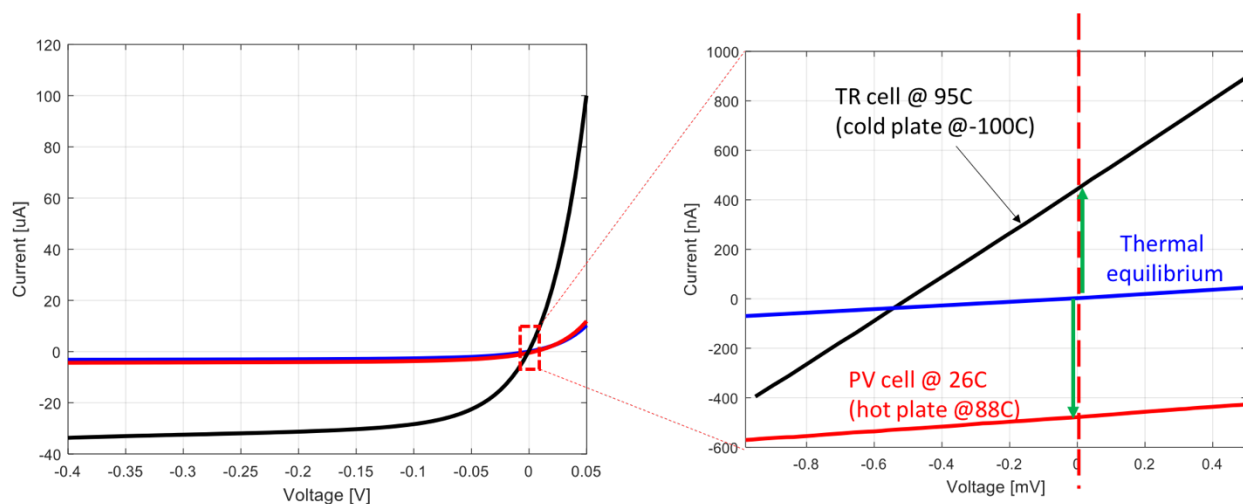


**Figure 11: I-V measurement of the cell under three conditions: 1) standard p-n junction under dark condition (blue curves); 2) thermo-radiative cell mode (black curves); 3) photovoltaic cell mode (red curves). Note the cell area is only  $0.01 \text{ mm}^2$ .**

Compare the thermo-radiative cell short circuit current for the two HgCdTe samples at ambient operating temperature, one can note that it changes from  $60 \text{ nA}$  (for  $E_g = 0.32 \text{ eV}$ ) to about  $3 \mu\text{A}$  (for  $E_g =$

0.21 eV). The corresponding current density changes from 6 A/m<sup>2</sup> to 300 A/m<sup>2</sup>. This is a 50X change. For  $E_g = 0.32$  eV cell, when the thermo-radiative cell temperature changes from ambient (295 K) to 368K (95°C), the short circuit current increases from 60 nA to 450 nA, as shown in Figure 11 (right) black curve.

To the best of our knowledge, this is the first experimental demonstration of the reversed current-voltage characteristics between a thermo-radiative cell and a photovoltaic cell. The demonstration clearly indicates the feasibility of using thermo-radiative cells for power generation. For example, we can integrate thermo-radiative cells with RPS radiators to harvest the low-grade waste heat, i.e., providing additional electric power for RPS. The relatively small short-circuit density shown in Figure 11 (right) is because the thermo-radiative cell used here for demonstration has a large bandgap (0.32 eV). Reducing this bandgap from 0.32 eV to 0.21 eV increased the short-circuit current by 50 times, for same operating condition.

## VI. Conclusion and Discussion

We have experimentally demonstrated a new technology concept, the thermo-radiative cell, as a new power generation method for deep space application. It naturally uses the ultra-cold deep space (3 K) as the heat sink, thus it is an ideal technology candidate for low-grade waste heat recovery. The predicted efficiency of thermo-radiative cells is significantly higher than thermoelectrics at peak power output, and can be even higher at reduced power output. Integrating thermo-radiative cells with radioisotope heating units (high-grade heat) or radioisotope power system (RPS) radiators (low-grade waste heat) could provide a new way to significantly increase the energy efficiency of Pu-238 or other radioisotope fuels.

Currently NASA has urgent needs to increase the efficiency of RPS [3], due to the short supply of Pu-238 which could put NASA's future space missions at risk [10]. As far as we know, NASA is pursuing two strategies to increase the efficiency of RPS [11]. One is developing the enhanced thermoelectric RPS (aka. e-MMRTG), the other one is developing dynamic RPS (such as Stirling, Brayton, or Rankine RPS). The expected efficiency for dynamic RPS is 25-30%, while future thermoelectric RPS is expected to have an efficiency of 8%. Obviously, in both technologies, there are significant amount of thermal energy dissipated via radiators as low-grade waste heat (ca. 325-475 K). Thermo-radiative cell technology can serve as the third strategy to increase the efficiency of RPS. It can be integrated with the RPS radiators to harvest electricity from the waste heat. While the waste heat being radiated into deep space via the thermo-radiative cells, part of the waste heat is converted into electricity. Due to the significant amount of waste heat and high efficiency of thermo-radiative cell, it could provide significant amount of additional power for the RPS.

Based on information from NASA's previous RPS programs, we assume the radiator area of a dynamic RPS is about 1.3 m<sup>2</sup>, and the radiator area of a thermoelectric RPS is about 0.79 m<sup>2</sup>. The actual radiator area that can be used for thermo-radiative cell integration should be larger than these conservative estimations. Based on the performance analysis results in section IV, we calculated the additional power gain and improved new efficiency as a function of the RPS radiator temperature, when thermo-radiative cells are integrated with RPS. As shown in Figure 12a, when thermo-radiative cells are integrated with a dynamic RPS, as the radiator temperature varies from 325 K to 400 K, the additional power gained from thermo-radiative cells varies from 30 W to about 96 W. As a result, the total thermal-to-electrical efficiency increases from 34% to 47%, compared to 28% of a dynamic RPS without thermo-radiative cells. Similarly, when thermo-radiative cells are integrated with a thermoelectric RPS, as the radiator

temperature varies from 415 K to 475 K, the additional power gained from thermo-radiative cells varies from 71 W to about 146 W. As a result, the total thermal-to-electrical efficiency increases from 10% to 14% (Figure 12b), compared to 6% of a thermoelectric RPS without thermo-radiative cells. Consequently, by integrating thermo-radiative cells with RPS radiators, both the efficiency improvement and additional power gain from the thermo-radiative cells are quite significant.

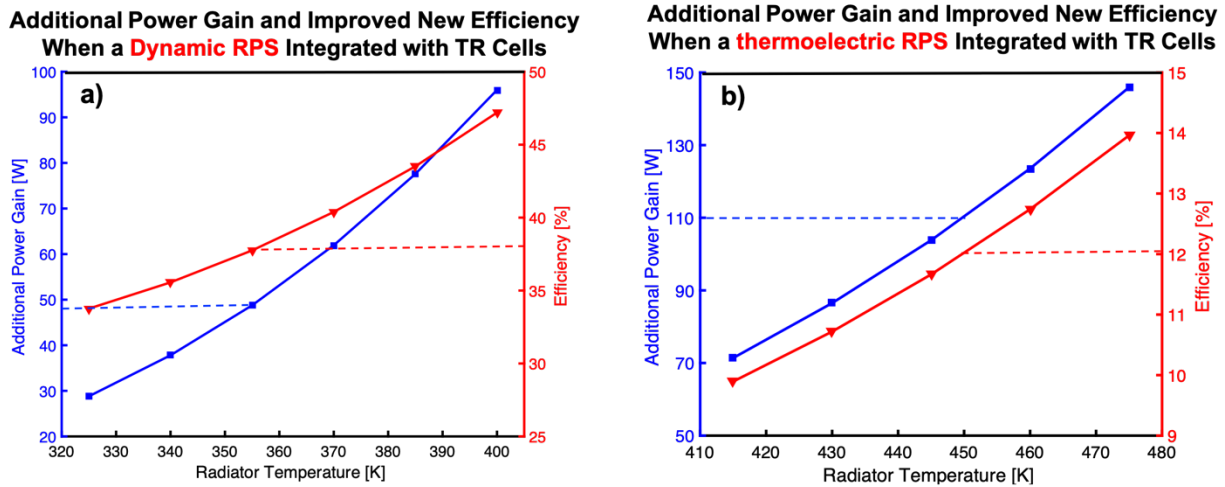


**Figure 12: Additional power gain and improved new efficiency when thermo-radiative cells are integrated with a (a) dynamic RPS or (b) thermoelectric RPS.**

In summary, thermo-radiative cell is a new waste heat recovery technology that is extremely suitable for space power applications. Usually it is difficult to harvest energy from low-grade waste heat since the temperature difference between the terrestrial ambient and low-grade waste heat is small, and the heat dissipation at low temperature is more difficult. However, in deep space, since thermo-radiative cell can easily make use of the cold universe as the heat sink (3 K to 150 K), it makes low-grade waste heat recovery much easier. In addition, it is passive with no moving parts, and does not require maintenance. It could potentially serve as an easy add-on to the radiator panels without changing the current RPS design. Our experimental demonstration and theoretical analysis indicate that combining thermo-radiative cells with either thermoelectric or dynamic RPS could significantly mitigate the stress on the short supply of Pu-238 radioisotope fuels. To the best of our knowledge, the reverse current-voltage characteristics between thermo-radiative cell and photovoltaic cell are experimentally demonstrated for the first time.

## Acknowledgements

This SBIR Phase I program was sponsored by NASA under contract No. NNX17CS05P. We would like to thank Wayne Wong of NASA Glenn, and Jean-Pierre Fleurial of NASA JPL for their helpful comments and suggestions on integrating thermo-radiative cells with NASA spacecraft.

## References

- [1] Schmidt, G.R., Sutliff, T.J., and Dudzinski, L.A. "Chapter 20 - Radioisotope Power: A Key Technology for Deep Space Exploration," *Radioisotopes – Applications in Physical Sciences*
- [2] News from Nuclear Science and Engineering Department, Oregon State University, "Rebuilding the Supply of Pu-238," <http://ne.oregonstate.edu/rebuilding-supply-pu-238>
- [3] "Space Exploration: Improved Planning and Communication Needed for Pu-238 and Radioisotope Power Systems Production," US Government Accountability Office Report, #GAO-17-673
- [4] Byrnes, S.J., Blanchard, R., and Capasso, R. "Harvesting renewable energy from earth's mid-infrared emissions," *Proc. Natl. Acad. Sci. USA*, 111, 3927-3932, 2014
- [5] Strandberg, R. "Theoretical efficiency limits for thermoradiative energy conversion," *J. Appl. Phys.*, 117, 055105, 2015
- [6] Hsu, W.-C., Tong, J.K., Liao, B., Huang, Y., Boriskina, S.V., and Chen, G. "Entropic and near-field improvements of thermoradiative cells," *Sci. Rep.*, 6, 34837, 2016
- [7] Shockley, W., and Queisser, H.J. "Detailed balance limit of efficiency of p-n junction solar cells," *J. Appl. Phys.* 32, 3, 510–519, 1961
- [8] Vos, A., and Pauwels, H. "On the Thermodynamic Limit of Photovoltaic Energy Conversion," *Appl. Phys.*, 25, 2, 119–125, 1981
- [9] Santhanam, P. and Fan, S. "Thermal-to-electrical energy conversion by diodes under negative illumination," *Phys. Rev. B*, 93, 161410, 2016
- [10] Witze, A. "Nuclear Power: Desperately seeking plutonium," *Nature*, 515, 484-486, 2015
- [11] Cataldo, R.L. and Bennett, G.L. "U.S. Space Radioisotope Power Systems and Applications: Past, Present and Future"